Space Perception Model which Generates Horopter

Taro Maeda
Mechanical Engineering Laboratory , MITI
Namiki 1-2, Tsukuba
Ibaraki, 305 Japan

Susumu Tachi
RCAST, The University of Tokyo
Komaba 4-6-1, Meguro-ku
Tokyo, 153 Japan

Abstract

One of the distinguished characteristics of human binocular visual space is the phenomenon which is represented as horopter and parallel/distance alleys. In this paper neural network models of space perception using binocular vision are presented to find out how the convergence angle and the bipolar latitude are mapped onto the depth sensation. One of the proposed models based on neural network model shows the characteristics of horopter and parallel/distance alleys which is similar to the human space perception. Structure of the model represents how the space perceptions generated in the human brain.

I. Introduction

Human space perception is highly relation to the visual sense, and knowledge of the characteristics of visual space perception is essential to research on three-dimensional human space perception. Human can perceive the location of a spot of light, and the distance between the spots by binocular vision even in complete darkness or a space where no spatially secondary cue is present. In these cases, the subjective straight line in the visual space to the objective point becomes the reference. Various psychological studies of this phenomenon are available, and the horopter, parallel/distance alleys are well known as the tools which represents its characteristics.

To investigate the characteristics, the head of the subject is fixed so as to make it immovable and all other cues in visual space are eliminated by the use of a dark room. Plural small spots of light are displayed in front of the subject in the horizontal plane at the height of the subject's eyes, and these light spots are moved so that they are seen by the subject to be on the same straight line longitudinally or laterally from the subject. The light spots arrebged on a physically-straight line is not necessarily subjectively straight, a difference whose parameters can be shown to be dependent on the distance from the subject.

That is, the arrangement of spots of light seen to be subjectively parallel with the frontal plane have a deviation from the corresponding physical straight line at a certain distance Xa from the subject. But when spots of light are arranged on a curve convex to the subject at a place farther than Xa or when they are arranged on a curve concave to the subject at a point nearer than Xa, they are observed subjectively as a straight line. This curve is called the horopter of Helmholtz (Fig. 1(a)) [1].
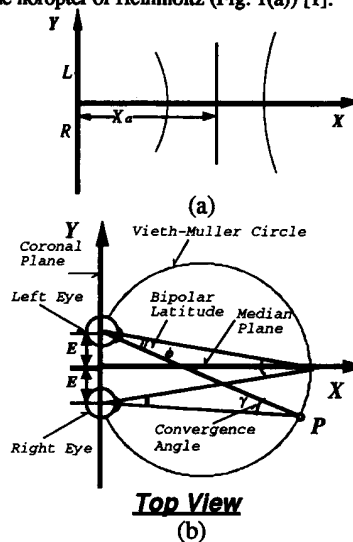

(a)

Top View
(b)

Fig.1. (a) Horopter curves for different fixations. This is a top view. L and R are left and right eye positions. (b) Convergence angle γ and bipolar latitude ϕ of a physical point P. Vieth-Muller Circle is a curve of constant convergence angle.

Horopter can be observed in each person. In general, different persons produce the different curves. However, each person has own horopter and parallel/distance alleys.

As for the curving of visual space, Luneburg has presented a geometrical theory of human space perception based on the Riemann and Lobatchevskii space having a certain curvature [2]. Based on the theory, Zajaczkowska [3] and Indow et al. [4] are studying on how to describe the curves.

The characteristics of the human visual space have been analyzed geometrically in detail as psychological phenomenon, but their origin has not been discussed. Originally, information used by humans actually in the process of space perception under the condition of horopter measurement is the orientation of the right and left eyeballs as they gaze at a spot of light, while perception of orthogonal coordinates, such as the parallel plane and parallel straight lines, is based on concepts developmentally acquired, rather than innate sensations. Therefore, it seems that some learning mechanism between them should exist.

In this paper, the characteristics of spatial vision are taken as those of a signal processing system in which the subject learns orthogonal space perception. Neural network models of space perception using binocular vision are introduced to construct the signal processing model which can describe space perception characteristics similar to those human shows in horopter and parallel/distance alley situations. Also through the consideration of signal processing using such models, signal processing mechanism in human space perception will be cleared [5].

II. A Space Perception Model with Horopter

A . Human space perception model

In general experiments of the horopter and parallel/distance alley, small spots of light on a horizontal plane which is at the subject's eye height are used as an index. Therefore, eye movement is limited to the horizontal in our models of the perception system.

Convergence angle γ and bipolar latitude ϕ are considered as information used for human space perception (Fig. 1(c)). Originally, right and left eye movements in binocular vision are not independent, but consist of conjugate eye movement of the same phase determining the bipolar latitude ϕ and convergent eye movements of the counter phase determining convergence of angle γ. These movements are considered to have a closer relationship with space perception than are the independent movements with directions α, β of the right and left eyes. This assumption is proved by the fact that the conjugate eye movement system and the convergent eye movement system are independent, and that eye muscle length determining α and β is not used directly to recognize the direction of view. The relationship of these two sets of signals is represented in the following two formulas.

$$\gamma = \pi - (\alpha + \beta)$$
$$\phi = (\beta - \alpha) / 2 \qquad (1)$$

When the distance between the two eyes is $2E$, the point $P = (x,y)$ can be represented with γ and ϕ as follows:

$$x = X(\gamma,\phi)$$
$$= \frac{E}{sin(\gamma)} \{ cos(\gamma) + cos(2\phi) \}$$
$$y = Y(\phi,\gamma)$$
$$= \frac{E}{sin(\gamma)} sin(2\phi) \qquad (2)$$

The space perception model is considered to be a system for learning to coordinate the relationship of (γ, ϕ) to (x,y), and on this basis the neural network models were formed.

In general horopter experiment, convergence* was used as a physiological cue which generates depth perception. The points on the Vieth-Muller Circle (hereafter VMC) shown in Fig.1(c) must appear equidistant because convergence angle γ is constant at these points, but the horopter is generally positioned outside the VMC in relation to the subject. This indicates that generation of depth perception does not depend only on the convergence angle γ, but also depends on the bipolar latitude ϕ. Therefore, our neural network models have to have some structure for interaction between these signals.

B. Physiological background

Perception of space is not purely visual but involves also the subject's body position and posture. It is the thought that input signals from various sense organs such as semicircular canals, the internal ear, etc. are integrated with visual sense and eye movement information in the brain. The portion of the brain most important for integral space perception is thought to be the parietal association cortex of the cerebral cortex [7]. In the cortex, the neural cells activated by gaze fixation on a small spot of light in space are found in area 7a of the posterior parietal association cortex**[8] These cells are a kind of visual fixation neuron (VF neuron). Reaction of the cells by gaze fixation on spots of light are classified into three types as follows:

---

* Originally, binocular parallax was thought to be an effective biological cue to depth perception under these conditions. However, when the subject can use only binocular parallax without eye movements for gazing, the horopter is not normal but coincident with VMC [6]. Therefore, it is supposed that binocular parallax is not concerned with the generation of the horopter.

**Obtained from experiments on alert monkey behavior and the existence of these VF neurons can be estimated in humans.

Type 1: Neurons with selectivity in different directions of gaze along vertical, horizontal and diagonal axes. Their discharge rates are monotonic increasing functions of deviation from the center.

Type 2: Neurons with selectivity in the depth of fixation. Their discharge rates are monotonic increasing or decreasing functions of distance from subject, regardless of the direction of the gaze.

Type 3: Neurons with selectivity both in the direction and distance of gaze fixation. Their discharge rates increase most by gaze fixation on the region previously specified three-dimensionally in space.

Selectivity of these neurons is controlled only by gaze direction and is less affected by background. It is considered that these cells have a close relationship with recognition of space location in eye movement [7].

C. Signal representation in biological systems by neural network models

Two signal representation models are discussed in this section. One uses the location of the firing cells and the other uses their firing rate.

There have been various discussions from the viewpoint of neural network model of how a biological system represents various signals in the brain. One of the problems discussed is whether the signal space is represented in the brain by the localization pattern of the firing cells or by the firing rate of the cells. That is, there are two concepts. In the first, a set of signals is assumed to form a signal pattern and the signals are represented by neural cells with selectivity to a particular set of values (Fig.2(a)). In the second, signal's values are represented by the firing rate of cells independent of each signal (Fig.2(b)). In practice, these representations are found in the brain as the output of a column of a sensory area and that of the sensory organ respectively, and either is said to be a general information representation mechanism.
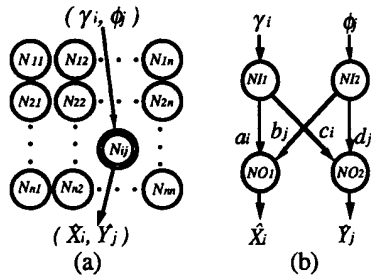

Fig.2. (a) A model of signal representation using localization of firing cells. (b) A model of signal representation using cell firing rate.

In addition, in models with different representation forms of signals, interaction among signals is also different. In the model of signal representation using localization of the firing cells shown in Fig.2(a), the set of input and output signals is combined through a cell, resulting in a kind of associative memory model. In the model of signal representation using the firing rate shown in Fig.2(b), the set of signals has mutual interactions resulting from repetitive addition of signals and conversion of the sum; this results in a structure which is a variety of multilayer network.

From the representation form of signals for the VF neurons described above, it was found that Type 1 and Type 2 correspond to the firing rate representation in Fig.2(b) and Type 3 to the localization representation of the firing pattern in Fig.2(a). Thus, both models are considered to be a potential model of human space perception. The models are classified as follows in terms of the structure of biological system information processing:

[Localization Model]

This is a model of signal representation using localization of firing cells.

In the case shown in Fig.2(a), it is possible to determine the mapping of two sets of two-dimensional signal spaces on a nerve field which is self-organized into two-dimensional topography (Appendix Fig.5(a))[9]. In this model, each of the cells arranged in a two-dimensional lattice represents a specific region of the signal space, and there is a uniform coordination throughout the lattice of input and output values for each specific region.

[Firing Rate Model]

This is a model of signal representation using cell firing rate.

In this model, the form of information processing is further classified into three kinds of models.

In the case shown in Fig. 2(b), γ and ϕ are represented by the firing rate of independent cells, and the effect on X and Y is thought to be additive. The reason interaction among signals is limited to addition is because signal processing in the neural network is basically an operation of weighted addition, as in the neuron model of MaCulloch-Pitts, which derives from various physiological phenomena. This assumption makes the model more natural. Such a model is represented in Fig.3(a). The structure of this model is given in the following formula:

$$\hat{X} = F_1(D_1(\gamma) + C_2(\phi)) ,$$
$$\hat{Y} = F_2(D_2(\phi) + C_1(\gamma)) \qquad (3.a)$$

This model is the prototype of models represented in Fig.3(b), (c) and (d), in which some nonlinear transfer functions concerning learning $(F_1, F_2, D_1, D_2, C_1, C_2)$ are limited.

Fig.3(b) represents the direct conversion model without mutually-correcting terms C_1, C_2 between γ and ϕ signals,

$\hat{X} = F_1(\gamma)$,

$\hat{Y} = F_2(\phi)$ (3.b)

Fig.3(c) represents the model in which mutually-correcting addition is made on the input signal space before conversion,

$\hat{X} = F_1(\gamma + C_2(\phi))$,

$\hat{Y} = F_2(\phi + C_1(\gamma))$ (3.c)

and Fig.3(d) represents the model in which mutually-correcting addition is made to the output signal space after conversion.

$\hat{X} = D_1(\gamma) + C_2(\phi)$,

$\hat{Y} = D_2(\phi) + C_1(\gamma)$ (3.d)

With these one localization model and three firing rate models, the solution of formula (2) can be derived, and the signal processing structure essential for defining human space perception characteristics can be investigated. Using these models, a neural network model for learning nonlinear transformation has been prepared (Appendix. Fig.5).

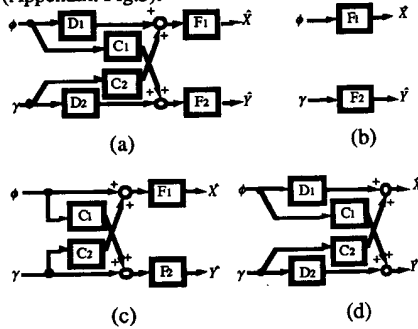(a)   (b)

(c)   (d)

Fig.3. (a) A prototype of firing rate models. (b) A firing rate model without mutually-correcting terms. (c) A firing rate model in which mutually-correcting addition is made to the input signal space before conversion. (d) A firing rate model in which mutually-correcting addition is made to the output signal space after conversion.

III. Experimental Method

In the experiment, learning was performed with the neural network models described above and represented in Fig.3(b), (c), (d) and Fig.5(a). When learning a point (X,Y), a central point $(X,0)$ on the parallel plane is made the reference to X, so that each transfer function is modified with the signals in Table 1. Then, equal learning can occur

for each model except in respect of the terms of mutually correcting addition.

Learning Unit	D_1	D_2	F_1	F_2	C_1	C_2
Fig..3(b) $C_1,C_2=0$ x	–	–	γ	ϕ	–	–
y'	–	–	X	Y	–	–
Fig..3(c) $D_1,D_2=1$ x	–	–	γ	ϕ'	γ	ϕ
y'	–	–	X	Y	$\gamma\text{-}\gamma$	$\phi'\text{-}\phi$
Fig..3(d) $F_1,F_2=1$ x	γ	ϕ	–	–	γ	ϕ
y'	X	Y	–	–	$Y\text{-}D_2(\phi)$	$X\text{-}D_1(\gamma)$
Fig..5(a) NerveField x	$x = (\gamma,\phi)$					
y'	$y'=(X,Y)$					

Table 1. Signals of each model for learning. Parameters are defined in Appendix. γ and ϕ are the convergence angle and the bipolar latitude at the learning point (X,Y). γ' is the reference convergence angle at $(X,0)$. ϕ' is the reference bipolar latitude at (X_d,Y) .

Respective constants are as follows:
$E = 34mm$
$X_d = 2000mm$
$n = 50$
$R = 3$
$a = a' = 0.2 \; exp(-m/5000)$ (4)
and the point of learning is within the region represented by the following formulas.
$\{ \phi \mid -0.15 \leq \phi \leq 0.15 \}$
$\{ X \mid 500mm \leq X \leq 2100mm \}$ (5)
This is the visual region where depth perception by convergence works most effectively.

When learning, the values of γ, ϕ are normalized so that the maximum and the minimum in the learning area become equal. Learning is compared after a number of learning trials corresponding to (number of cells included in the nerve field)/(number of cells learning at any one time) for each model. Learning of $mmax = 20,000$ trials was performed in the firing rate model. Learning of $mmax = 150,000$ trials was performed in the localization model.

IV. Experimental Results

As a result of learning with the model shown in Fig.5(a) and Fig.3, the following horopters were obtained. They are shown in Fig.4. Dotted lines are VMC for control.
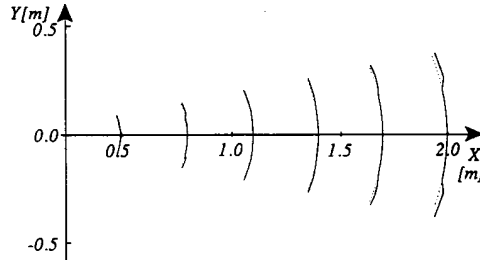
These figures are shown with the points plotted using the method of adjustment to those of a human subject.

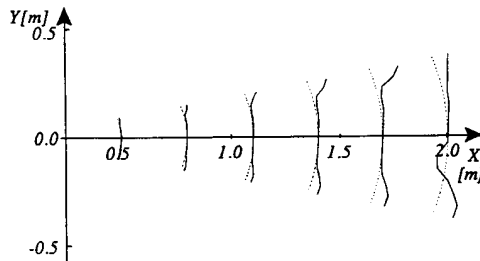The horopter tendencies for human subjects are as follows:
1) The horopter becomes concave to the subject at the near point.
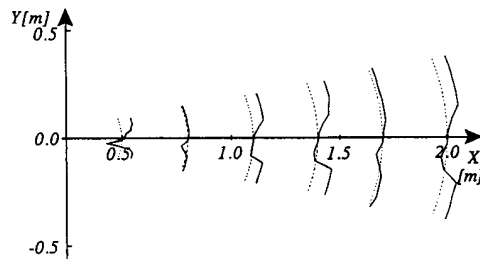2) The horopter becomes convex to the subject at the far point.
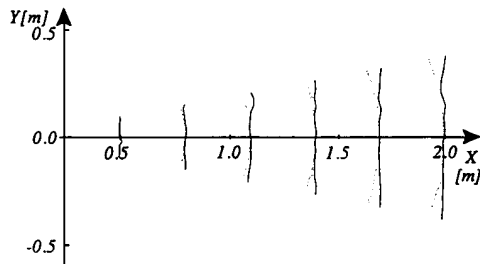
(a) The localization model.

(b) The firing rate model without mutually-correcting terms.

(c) The firing rate model with mutually-correcting addition made to the input signal space.

(d) The firing rate model with mutually-correcting addition made to the output signal space.

Fig.4. Horopters of models. Dotted lines are VMC for control.

3) The curvature varies continuously with the distance from the subject.
4) The curvature becomes zero at distance Xa (Fig.1(a)). Xa is usually about 1000 to 1500 mm.
5) The curvature changes from concave to convex only once. There is no change from convex to concave.
6) The horopter is symmetric about the median plane.
7) The horopter is always positioned outside the VMC in relation to the subject.

(1) to (3) of these tendencies are represented in Fig.1(a).

Concerning the firing rate model, Fig.4(b) shows the direct conversion model in which the mutually correcting terms of γ and ϕ, C_1 and C_2 are not present, and the horopter showed almost VMC. This was because depth perception was dependent only on the convergence angle information in this model ; this result was expected.

Fig. 5(c) represents the model in which mutual correction is made before conversion. In this model, the curvature of the horopter varied from concave to convex depending on the distance from the subject, and the horopter showed a shape similar to a human subject's. Depth Xa, matching the objective parallel plane was observed in the vicinity of 1000 to 1500 mm ; this is also similar to the value measured for subjects.

Fig. 5(d) shows the model in which mutual correction is made after conversion. In this model, the curvature of the horopter varied from convex to concave to flat, and was therefore a different shape than that of a human subject : a horopter curvature varying from convex to concave with distance from the subject is never observed in human subjects.

In the localization model shown in Fig.4(a), the output was most coincident among the models with the orthogonal coordinates. Especially in the vicinity of $\phi=0$, almost complete coincidence was seen, and there was no distorted inclination. However, on this point, this model's results differ from those of the human subjects.

V. Considerations

From the results of the horopter experiments, it was found that the firing rate model in which mutual correction is made before conversion with a unilateral space learning area best modelled human space perception among all the models. On this basis, the signal processing structure of the coordinate conversion processing system for human space perception is considered as follows.

At first, the firing rate model and the localization model are compared. The output of the localization model coincides with the orthogonal coordinate system while the output of the firing rate models does not. This is because the localization model functions as something akin to associative memory and has more general learning ability for transformation of coordinate systems. However, the output of this model coincides too exactly with the orthogonal coordinate system to accurately model human space perception . Therefore, although the human brain does have localization pattern representation, which is the more general coordinate transformation system, its representation form is evidently not concerned with generating the subjective results found in the horopter and alleys experiments.

Furthermore, from formula (2), the following relationship can be obtained.

$$\frac{\partial X}{\partial \gamma} = -\frac{E\ \{\ 1\ +\ cos(\ 2\phi\ )\ cos(\ \gamma\ )\ \}}{sin^2(\gamma)}$$

$$\frac{\partial X}{\partial \phi} = -\frac{2E\ sin(\ 2\phi\ )}{sin(\gamma)}$$

$$\frac{\partial Y}{\partial \gamma} = -\frac{E\ sin(\ 2\phi\ )\ cos(\ \gamma\ )}{sin^2(\gamma)}$$

$$\frac{\partial Y}{\partial \phi} = \frac{2E\ cos(\ 2\phi\ )}{sin(\gamma)} \tag{6}$$

By this, the following relationship is obtained over most of the recognition area,

$$\frac{\partial X}{\partial \gamma} < 0\ , \qquad \frac{\partial Y}{\partial \phi} < 0 \tag{7}$$

and there are also the following relationships of expected values over the recognition area.

$$E\left(\frac{\partial X}{\partial \phi}\right) \cong E\left(\frac{\partial Y}{\partial \gamma}\right) \cong 0$$

: When E(X) is X's expected value. (8)

The high correlation between signals represented by the monotonic relationship between dX and $d\gamma$, dY and $d\phi$ may indicate the generation of more direct connections between signals. The possibility of the relationship producing direct connections between cells without there being characteristic cells for a space area (cf. Type 3 of VF neurons whose discharge rates increase most by gaze fixation of a region specified three dimensionally in space) is shown by results such as that of this experiment that one of the firing rate models best represents actual human space perception .

In this paper, the signal space is considered as two-dimensional, but in the firing rate model, three-dimensional models can be made as the similar models to two-dimensional models, by considering Type.1 VF neuron with vertical directional selectivity of gaze. In the localization model, a nerve field with three-dimensional topology is required for preserving topology, and

as the topology in the nerve field in the brain is two-dimensional, the application of model will generate a problem. As for deficient order, it can be represented by using a hypercolumn model but a portion of the topology may be broken. Thus in this respect also the localization model may not be suitable as a three-dimensional space perception model.

Next, the interaction structures of the firing rate models are compared. The difference between Fig.3(c) and Fig.3(d) in the firing rate model is that additive mutual correction processing between signals is performed before conversion or after it. This means that the correction processing is performed in the signal space of the subjective orthogonal coordinate system (X,Y) in the model of Fig.3(d), but it is performed in the signal space of the eye movement signal (γ,ϕ) in Fig.3(c).

The results of the horopter experiment strongly support the structure represented in Fig.3(c) as a human depth perception model. From this tendency, it is possible that the processing system for the generation and compensation of higher-order conceptions, such as the frontal parallel plane, acquired later in the development of space perception performs information processing in the form of a primary sensing signal (i.e. eye movement), if the scale accuracy on the conceptive quantity is not essential to a certain perception. This raises the possibility that the integration and processing of positional information in visual space perception are performed in the eye movement signal space or in the signal space extremely near it, because convergence is a main cue of absolute depth in visual space perception and other cues of relative depth, such as binocular parallax, are subsequently integrated with the absolute depth information by developmental learning.

This conclusion supports the hypothesis that humans may not use an abstract signal form for global space representation in information processing when integrating various sense modalities in space perception. There is corroborative physiological evidence to support this conclusion [10].

VI. Conclusion

In this paper, it is considered that the horopter and parallel/distance alleys, which have been thought to be phenomena in psychology, are actually structural characteristics of signal processing in the human neural network, resulting from the learned transformation of binocular eye movement information into a subjective orthogonal coordinate system. Psychological and physiological knowledge offers several space perception models with different signal processing

structures. In the learning simulation experiments, the models generated horopter, parallel alley, and distance alley results which were similar to those of a human being.

On the basis of these results, it can be concluded that the signal processing system in human space perception uses the essential signal space for each perception as the signal space for interaction between signals.

APPENDIX:
A NEURAL NETWORK MODEL FOR LEARNING NON-LINEAR CONVERSION

A neural network model for learning the transformation of (γ,ϕ) to (X,Y) in the localization model is shown in Fig.5(a). The model used in this study consists of two input cells, which are internal cells arranged in an $n \times n$ lattice with two output cells. The internal cells form a two-dimensional nerve field with lateral inhibition. The model forms a two-dimensional topography on the nerve field and a desired non-linear continuous function between input and output signals by learning of Kohonen's topology-preserving mapping [9][11][12].
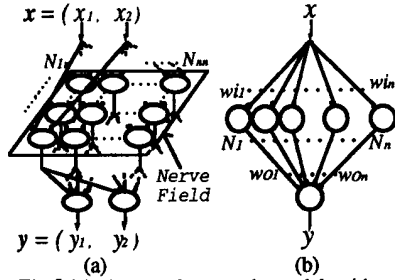

Fig.5.(a) A neural network model with two-dimensional topology preserving mapping. (b) A neural network model with one-dimensional topology preserving mapping.

Cell N_{ij} of the i column and j row in the $n \times n$ nerve field has input weight wi_{ij} to input vector x, and its activation a_{ij} is represented in this formula.

$$a_{ij} = \frac{1}{1+//x-wi_{ij}//} \quad (9)$$

Provided that $//$ represents the two-dimensional norm, the cell group S_{fg} actually firing, (the center of which is the most activated cell N_{fg}), is defined as follows:

$$S_{fg}=\{N_{ij}/\ f-R\leq i \leq f+R\ and\ g-R\leq j \leq g+R,\ when\ a_{fg}=max\{a_{ij}/\ i,j=1,2,\cdots,n\} \quad (10)$$

Here, R is the activation interaction radius in the nerve field.

Provided S_{fg} is adjacent $(2R+1)^2$ cell groups [12], which forms output vector y by synaptic weight wo_{ij}.

$$y = \sum_{N_{ij}\in\ S_{fg}} wo_{ij}\ /(2R+1)^2 \quad (11)$$

Similarly, learning occurs only for the cells firing. That is, learning occurs for synaptic weight wi_{ij} of cell N_{ij} comprised in S_{fg} with input x,

$$\Delta wi_{ij}= \alpha\ (x-wi_{ij}) : if\ N_{ij}\in S_{fg}$$
$$= 0 \qquad\qquad : otherwise \quad (12)$$

and similarly for synaptic weight wo_{ij} with correct output y'

$$\Delta wo_{ij}= \alpha'\ (y'-wo_{ij}) : if\ N_{ij}\in S_{fg}$$
$$= 0 \qquad\qquad : otherwise \quad (13)$$

In the formulas, α and α' are learning coefficients. When learning has sufficiently progressed, correct input and output are represented in the following formula,

$$y'=y=f\ (x)\ ,\quad x= (x1,x2)$$
$$x1_{min}\leq x1 \leq x1_{max}, x2_{min}\leq x2 \leq x2_{max} \quad (14)$$

and the respective weights of the cell groups are converged as follows,

When $wi_{ij} = (\ wi_{ij}1\ ,\ wi_{ij}2\ )$,

$$x1_{min}\leq wi_{i1}1\ <wi_{i2}1\ <\cdots<wi_{in}1\ \leq x1_{max}$$
$$or\ x1_{min}\geq wi_{i1}1\ >wi_{i2}1\ >\cdots>wi_{in}1\ \geq x1_{max},$$
$$x2_{min}\leq wi_{1j}2\ <wi_{2j}2\ <\cdots<wi_{nj}2\ \leq x2_{max}$$
$$or\ x2_{min}\geq wi_{1j}2\ >wi_{2j}2\ >\cdots>wi_{nj}2\ \geq x2_{max} \quad (15a)$$

or are converged in the following:

$$x1_{min}\leq wi_{1j}1\ <wi_{2j}1\ <\cdots<wi_{nj}1\ \leq x1_{max}$$
$$or\ x1_{min}\geq wi_{1j}1\ >wi_{2j}1\ >\cdots>wi_{nj}1\ \geq x1_{max},$$
$$x2_{min}\leq wi_{i1}2\ <wi_{i2}2\ <\cdots<wi_{in}2\ \leq x2_{max}$$
$$or\ x2_{min}\geq wi_{i1}2\ >wi_{i2}2\ >\cdots>wi_{in}2\ \geq x2_{max} \quad (15b)$$

and topography reflecting the topology of input x is formed [9].

$$wo_{ij}\cong f\ (wi_{ij}) \quad (16)$$

This time, the respective cells react characteristically to specific regions in the input-output space, and a desired non-linear continuous function $y=f(x)$ is established between input and output.

Further, by utilizing this characteristic, a one-dimensional model (Fig.5(b)), forming a one-dimensional topography of one input and one output, is used as a neural network to learn the

respective non-linear functions of the firing rate models. This time, formulas corresponding to expressions (12) to (19) in the one-dimensional model are represented in the following formulas (12)' to (19)'.

$$a_i = 1/(1 + |x - wi_i|) \qquad (11)'$$

$$S_f = \{N_i | f\text{-}R \leq i \leq f + R\}$$
$$\text{when } a_f = max\{a_i | i = 1, 2, \cdots, n\} \qquad (12)'$$

$$y = \sum_{N_i \in S_f} wo_i/(2R+1)^2 \qquad (11)'$$

$$\Delta wi_i = \alpha (x - wi_i) : if \ N_i \in S_f$$
$$= 0 \qquad : otherwise \ (12)'$$

$$\Delta wo_i = \alpha' (y' - wo_i) : if \ N_i \in S_f$$
$$= 0 \qquad : otherwise \ (13)'$$

$$y' = y = f(x) \ , \ x_{min} \leq x \leq x_{max} \qquad (14)'$$

$$x_{min} \leq wi_1 < wi_2 < \cdots < wi_n \leq x_{max}$$

$$or \ x_{min} \geq wi_1 > wi_2 > \cdots > wi_n \geq x_{max} \qquad (15)'$$

$$wo_i = f(wi_i) \qquad (16)'$$

REFERENCES

[1] H.V.Helmholtz, "Treatise on Psychological Optics," Optical Society of America, vol.3, pp.482-, 1925.

[2] R.K.Luneburg, "The Metric of Binocular Visual pace," Journal of the Optical Society of America, vol.40, no.10, pp.627-642, 1950.

[3] A.Zajaczkowska, "Experimental Test of Luneburg's Theory.Horopter and Alley Experiments," Journal of the Optical Society of America, vol.46, no.7, pp.514-527, 1956.

[4] T.Indow, "An Approach to Geometry of Visual Space with No A Priori Mapping Functions : Multidimensional Mapping According to Riemannian Metrics," Journal of mathematical psychology, vol.26, pp.202-236, 1982.

[5] T.Maeda, S.Tachi, "Space Perception Model which Generates Horopter," Transactions of the Society of Instrument and Control Engineers, vol.25, no.10, pp.1111-1118, 1989. (In Japanese)

[6] K.Sigeoka, "Experimental studies on position constancy," In Y.Akishige(Ed.), Experimental Researches on the Structure of the Perceptual Space V. Bull.Fac.Lit.Kyushu Univ., no.9, pp.189-228,1965.

[7] M.Critchley,"The Parietal Lobe," Hafner, 1953.

[8] H.Sakata, H.Sibutani and K.Kawano, "Spatial Properties of Visual Fixation Neurons in Posterior Parietal Association Cortex of the Monkey," Journal of Neurophysiology, vol.43, pp.1654-1672, 1980.

[9] Y.Sakaguchi, M.Zama, T.Maeda, K.Nakano and T.Ohmori, "Cooperation of Sensory System and Motor System," Proceeding of the 29th SICE Annual Conference, vol.1, pp.73-74, 1987. (In Japanese)

[10] D.N.Levine,K.J.Kaufman, and J.P.Mohr, "Inaccurate Reaching Associated with a Superior Parietal Lobe Tumor," Neurology, vol.28, pp.556-561, 1978.

[11] A.Takeutchi and S.Amari, "Formation of Topographic Maps and Columnar Microstructures in Nerve Fields," Biol.Cybern., vol.35, pp.63-72, 1979.

[12] T.Kohonen, "Self-Organized Formation of Topologically Correct Feature Maps," Biol.Cybern., vol.43, pp.59-69, 1982.